JOURNAL OF THE KOREAN ASTRONOMICAL SOCIETY
35: 87 ~ 95, 2002

DYNAMICAL EVOLUTION IN THE OPEN CLUSTER NGC 6819

YONG-WOO KANG[1,2] AND HONG BAE ANN[1]
[1] Department of Earth Sciences, Pusan National University, Pusan 609-735, Korea
E-mail: ywkang@galaxy.yonsei.ac.kr
[2] Department of Astronomy, Yonsei University, Seoul, 120-749, Korea
E-mail: hbann@cosmos.es.pusan.ac.kr
(Received May 6, 2002; Accepted Jun. 10, 2002)

ABSTRACT

We have conducted VI CCD photometry of the open cluster NGC 6819 in order to understand the effects of dynamical evolution in old open clusters. Our photometry covers $18' \times 18'$ on the sky, centered on the cluster, which seems to cover the whole cluster field. Our photometry reaches down to $V \approx 20.5$, which allows us to analyze the luminosity function and spatial distribution of stars brighter than $M_V \approx 8.5$. There is a clear evidence for mass segregation in NGC 6819, i.e., the giants and upper main-sequence stars are concentrated in the inner regions, whereas the lower main-sequence stars distribute almost uniformly throughout the cluster. The luminosity function of the main-sequence stars of NGC 6819 is almost flat. The flat luminosity function indicates that a large number of low mass stars has escaped from the cluster unless its initial mass function is much different from the Salpeter type ($\Phi(m) \propto m^{-(1+x)}, x = 1.35$).

Key words: open clusters: individual (NGC6819)— luminosity function, mass function

I. INTRODUCTION

NGC 6819 is an open cluster, located near the Galactic plane ($\alpha_{1950} = 19^h39^m36^s$, $\delta_{1950} = +40°04'$; $l^{II} = 73.°98, b^{II} = 8.°47$. The Trumpler class is I1r (Lyngå 1987), which means that it is a highly concentrated and rich cluster with small brightness range. The angular diameter of NGC 6819 is known to be small, ($D \approx 5'$; Lyngå 1987) but the visual inspection of the Digital Sky Survey (DSS) images shows that the diameter of NGC 6819 is much larger than $5'$.

Earlier photometric studies of NGC 6819 indicated that it is an old open cluster, similar to M67 (Burkhead 1971; Lindoff 1972; Auner 1974). Recent estimate of the cluster age by Rosvick & VandenBerg (1998) using the isochrone fitting to the color-magnitude diagram (CMD) of NGC 6819 based on BV CCD photometry shows that the age of NGC 6819 is ~ 2.4 Gyr which is similar to that of Lindoff (1972) but slightly younger than that of Kaluzny & Shara (1988) who estimated the cluster age as 4 Gyr using the morphological age ratio (MAR) method (Anthony-Twarog & Twarog 1985).

There have been several photometric studies of NGC 6819 since the photoelectric and photographic photometry of Burkhead (1971), including the recent BV CCD photometry by Rosvick & VandenBerg (1998). However, most of the previous studies are focused on the photometric properties of the individual stars (Gillam 1993) or the cluster parameters such as distance, reddening, and age (Canterna et al. 1986; Kaluzny & Shara 1988).

The metallicity of NGC 6819 is known to be similar to the solar metallicity, [Fe/H] ≈ 0.0, from moderate resolution spectroscopy of cluster giants (Friel & Janes 1993; Thogerson, Friel, & Fallon 1993). Recent estimates of the metallicity of NGC 6819 by high resolution spectroscopy of the red clump stars (Bragaglia et al. 2001), confirms that NGC 6819 has a near solar metallicity, [Fe/H] $=0.09 \pm 0.03$.

Dynamical properties of open clusters are difficult to be understood due to lack of kinematical data for most of open clusters. However, it is possible to draw some information about the dynamical evolution of open clusters by statistical analysis of the spatial distribution of cluster stars and their luminosity functions, by employing photometric membership for individual stars (Ann & Lee 2002). NGC 6819 seems to be one of the best targets for dynamical studies of open clusters owing to the age and the richness of the cluster.

Recently, Kalirai et al. (2001) conducted a deep BV photometry of NGC 6819 using CFH12K CCD from which they analyzed the luminosity function and mass function as well as the cluster white dwarfs. Thanks to the wide field coverage of the CFH12K CCD, they were able to determine the cluster extent ($R \sim 9.'5$) by star counts, which is about two times larger than previous estimates (Lyngå 1987). They also showed that low mass stars predominate in the outer regions of the cluster, indicating mass segregation due to dynamical evolution. The present study using the VI CCD photometry of NGC 6819 confirms the mass segregation found by Kalirai et al. (2001) and suggests other evidences for the dynamical evolution in NGC 6819. The

Corresponding Author: H. B. Ann

dependence of the degree of mass segregation on the age of the cluster will be discussed in our forthcoming paper (Kang & Ann 2002). In §II, we describe the observations and data reduction, and the resulting CMD and isochrone fittings are presented in §III. The structural properties and the luminosity functions are analyzed in §IV and §V, respectively. The summary and discussion are given in the final section.

II. OBSERVATION AND DATA REDUCTION

(a) Observations

The photometric observations of NGC 6819 were carried out by using a SITe CCD Camera attached to the 1.8m Plasket Telescope of Dominion Astrophysical Observatory (DAO), on 1997, August 4. We used standard Johnson- Cousins V and I filters. The CCD camera has 1024 × 1024 pixels with a pixel size of 24 μm which corresponds to $0.''55$ on the sky. The field of view of the CCD is $9.'2 \times 9.'2$.

We observed a region of about $18' \times 18'$, centered on NGC 6819, which consists of five CCD frames. The individual frames are observed with sufficient overlapping regions for the zero point adjustment. We used a pair of short and long exposure times for each filter to avoid loss of stars due to saturation. Landolt (1992) standard field PG 2331+055 and a standard field in NGC 7790 (Christian et al. 1985) were observed during the night for the transformation to the standard photometric system. The observational log is given in Table 1. Fig. 1 shows the final mosaic image of the observed field where stars are plotted by field circles whose radii are proportional to their brightness. We see that brighter stars, i.e., large circles, are more abundant in the inner regions.

(b) Data Reduction

We have reduced the CCD images using the IRAF package following the standard procedures, including the overscan correction, bias subtraction, and flat-fieldings. We used the twilight sky as the source of the flat fields. The instrumental magnitudes of the stars in the cluster field are determined by PSF photometry using IRAF/DAOPHOT but the instrumental magnitudes of standard stars are derived by the aperture photometry. The aperture correction was applied to the magnitudes from the PSF photometry using the aperture determined by the growth curve method.

Table 1. Observational data for NGC 6819

Field	Filter	Exposure(sec)	Seeing(arcsec)
Center	V	10, 900	2.8, 2.6
	I	10, 600	2.2, 2.4
SW	V	10, 800	2.8, 2.7
	I	10, 600	2.4, 2.5
SE	V	10, 800	2.0, 2.3
	I	10, 600	2.0, 2.6
NW	V	10, 800	2.1, 2.6
	I	10, 600	2.7, 2.8
NE	V	10, 200	2.5, 2.6
	I	10, 200	2.4, 2.5

The instrumental magnitudes were transformed to the standard system by using the transformation equations derived from the photometry of the standard stars,

$$V = v - 0.252X + 0.029(V - I) - 2.120$$
$$I = i - 0.212X + 0.062(V - I) - 2.446$$

where the capital letters represent the standard magnitudes and the lower case letters stand for the instrumental magnitudes with X as air mass. Fig. 2 shows the residuals of the transformation equations. The mean residuals are $\Delta V = 0.042$, $\Delta I = 0.037$, and $\Delta(V - I) = 0.038$, respectively.

For bright stars, we used the magnitudes from the short exposure images, while we used the long exposure images for faint stars. The zero point shift was allowed for different frames using the stars in the overlapped regions. The weighted mean magnitudes were adopted for the stars in the overlapped regions in the mosaicked images.

Fig. 3 shows the comparison of the present photometry with that of Lindoff (1972). Owing to the lack of I magnitudes in Lindoff (1972)'s photometry, we plotted only the V-magnitude difference between the present photometry and that of Lindoff (1972), ΔV, against V and $V - I$ of the present photometry. There seems to be no systematic trend with magnitudes and colors between the two photometry but there is a zero point shift of 0.05 mag in V with a mean dispersion of 0.03 mag, in the sense that our photometry is brighter than that of Lindoff (1972).

III. COLOR-MAGNITUDE DIAGRAM

Fig. 4 shows the V vs $V - I$ CMD of all the stars identified in the mosaicked image of NGC 6819. The number of stars plotted in Fig. 1 is 6570. Although there seems to be a heavy contamination of field stars, the main-sequence of NGC 6819 is distinct down to $V \approx 20$. The turnoff point of the main-sequence is well defined and there are a large number of stars in the giant branch, especially in the clump region. Thus, the CMD of NGC 6819 exhibits a typical CMD morphology of old open clusters.

We estimated the cluster parameters by fitting the Padova isochrones (Bertelli et al. 1994) to the stellar distributions in the V vs $V - I$ CMD of the central region ($r \leq 5.'5$) of NGC 6819. Because the recent estimates of the metallicity of the cluster indicate that NGC 6819 has metallicity between [Fe/H]

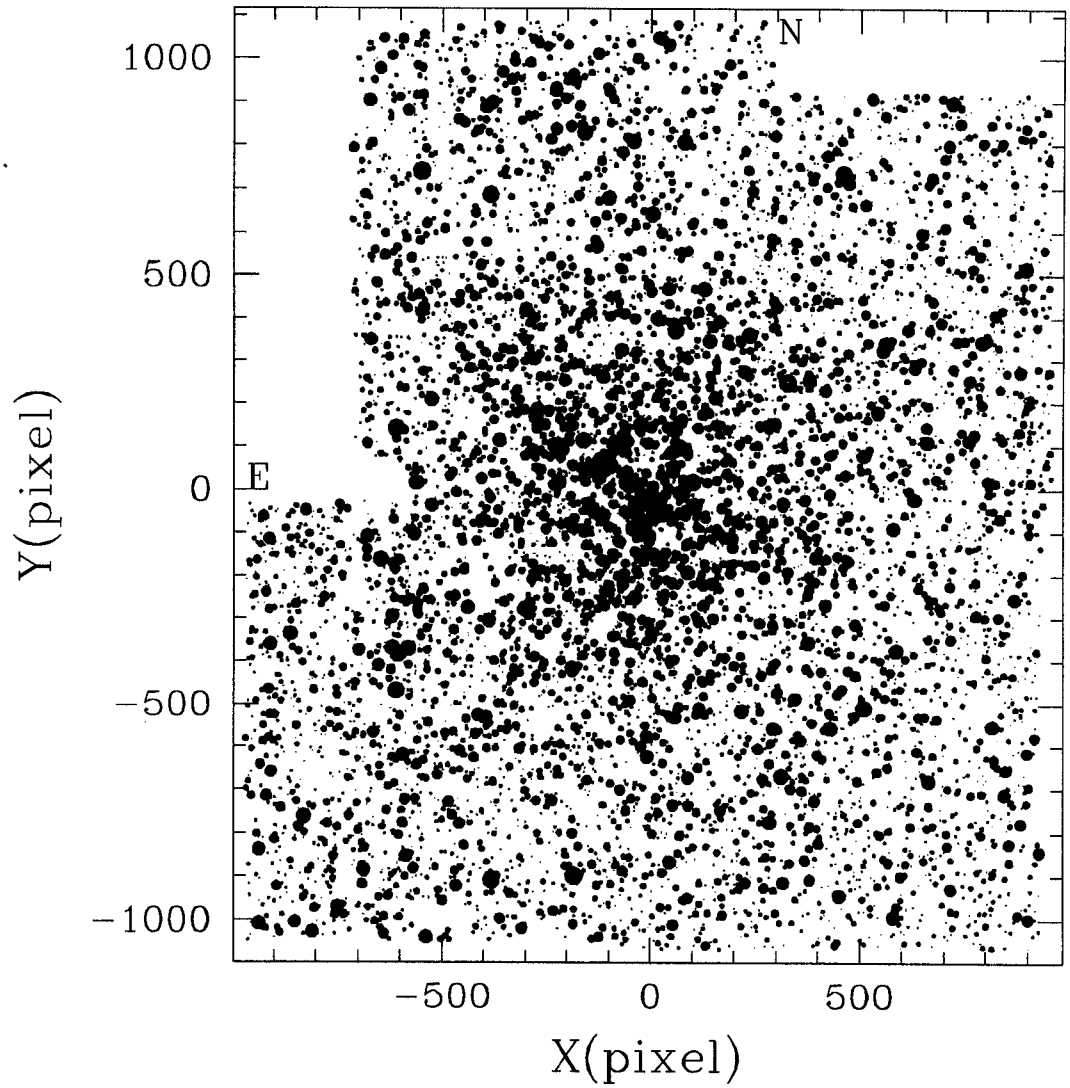

Fig. 1.— The V filter mosaic image of NGC 6819. The size of the image is $18' \times 18'$. North is up and east is to the left.

$\approx$ 0.0 and [Fe/H] $\approx$ 0.09, we fitted the reddening, distance modulus, and age, simultaneously, by fixing the metallicity as [Fe/H] = 0.07. Fig. 4 shows the best fit isochrone, which gives the cluster parameters as $E(B-V) = 0.10 \pm 0.03$, $(m-M)_0 = 11.8 \pm 0.2$, and $log(t) = 9.4 \pm 0.1$, with [Fe/H]=0.07. In the fitting process, we assumed $E(V-I) = 1.25E(B-V)$ (Dean et al. 1978) and the total to selective absorption ratio R as 3.0. Our estimate of distance modulus is in a good agreement with those of Rosvick & VandenBerg (1998) but it is 0.3 mag smaller than that of Kalirai et al. (2001). Because our estimate of $E(B-V)$ is the same as that of Kalirai et al. (2001) and there seems to be virtually no difference in the zero points of the two photometry, it is unclear what makes the difference in the derived distance modulus.

IV. STRUCTURAL PROPERTIES

We examined the spatial distribution of stars in the field of NGC 6819 using DSS data along with the present photometry. We counted stars in running annuli around the center of the cluster using the mosaicked image in Fig. 1 and the DSS image of $30' \times 30'$, centered on the cluster.

(a) Surface Density Distribution

We determined the cluster center by counting stars in vertical and horizontal strips across the images. The width of the strips was selected to be 70 pixels to suppress the effect of random fluctuations of the stellar density. After determining the position of the cluster center, we determined the surface number density along

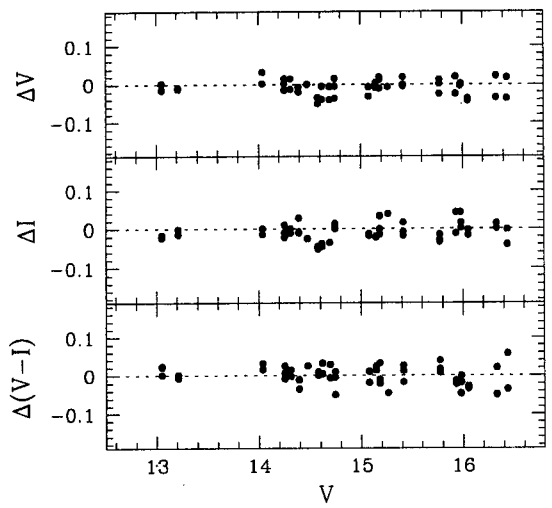

Fig. 2.— The residuals (standard magnitudes minus transformed magnitudes) of the standard transformation for V and I. There seems to be no non-linear pattern in the transformations. The mean residuals in V, I, and $V-I$ are 0.042, 0.037, 0.038, respectively.

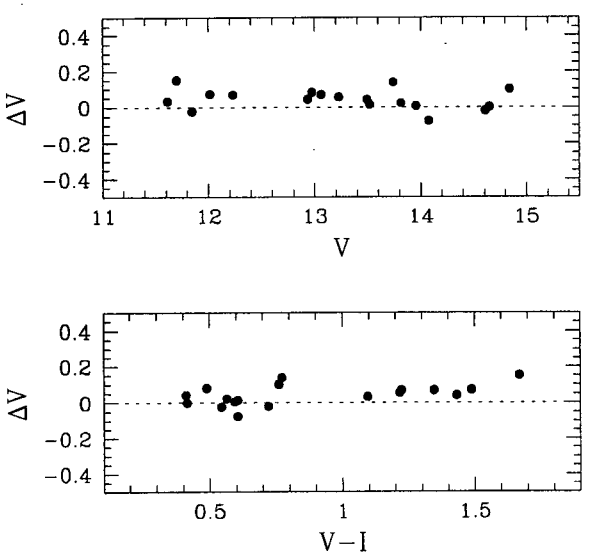

Fig. 3.— Comparison of the present photometry with that of Lindoff (1972). There is no systematic difference between the two photometry.

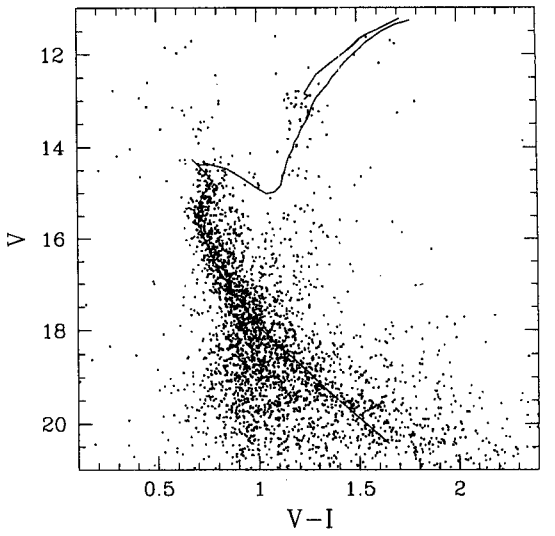

Fig. 4.— V vs $V-I$ CMD of the stars in the field ($\sim 18' \times 18'$) of NGC 6819. We see the populous clump stars. The turn-off point is well defined. The solid line represents the isochrone of $log(t) = 9.4$ and [Fe/H]=0.07 with a distance modulus of $(m-M)_0 = 11.8$ and $E(B-V) = 0.10$.

the radius by counting the number of stars in concentric annuli whose width is 35 pixels wide. Fig.5 shows the stellar surface density as a function of the cluster radius. The surface density from the present CCD image (top panel) decreases continuously outward, whereas that from the DSS image (bottom panel) decreases up to $r \approx 9'$ and becomes flattened thereafter. This indicates that NGC 6819 extends to $r \approx 9'$, which is about two times larger than the cluster size thought previously. But, the present estimate of the cluster radius is in a good agreement with the recent estimate by Kalirai et al. (2001), $R = 9.'5 \pm 1.'0$. The density difference between the density plots in Fig. 5 is due to the different limiting magnitudes of the two images as well as the severe saturation of the bright stars in the DSS image. The limiting magnitude of the CCD image is $V \sim 20.5$ whereas that of the DSS image is $V \sim 18$.

The surface density distribution of the stars in the field of NGC 6819 suggests that NGC 6819 consists of three components; core ($r < 1.'6$), inner corona ($1.'6 \leq r < 5.'5$) and outer corona ($5.'5 \leq r < 8.'8$). The three component characteristics of open cluster is reported by Nilakshi & Sagar (2002) for NGC 2099 although their nomenclature is slightly different from ours. They used corona 1 and corona 2 for the inner corona and outer corona, respectively. The core resembles the core of the isothermal sphere which is well represented by the King model (1962). The surface density outside the high density core decreases slowly up to $r \approx 5.'5$ and drops abruptly at the edge of the inner corona. It seems quite natural to think it as the cluster radius because the stellar density outside this radius is too low to be detected easily. This is the reason why most

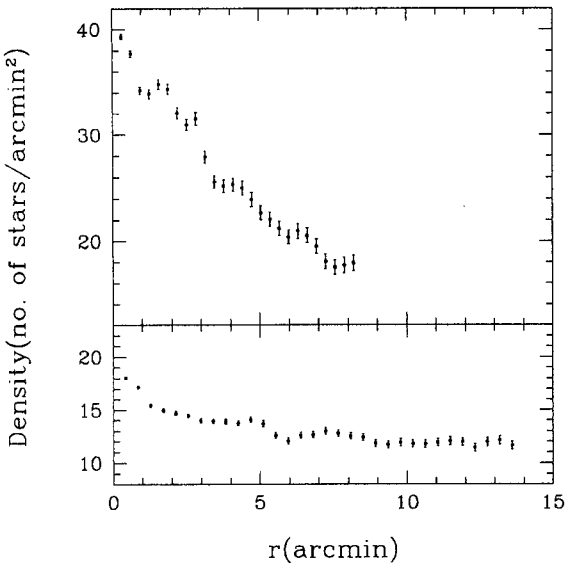

Fig. 5.— Radial surface density distribution of stars in the field of NGC 6819. The upper panel is the surface density from the present photometry and the lower panel is that from the DSS image.

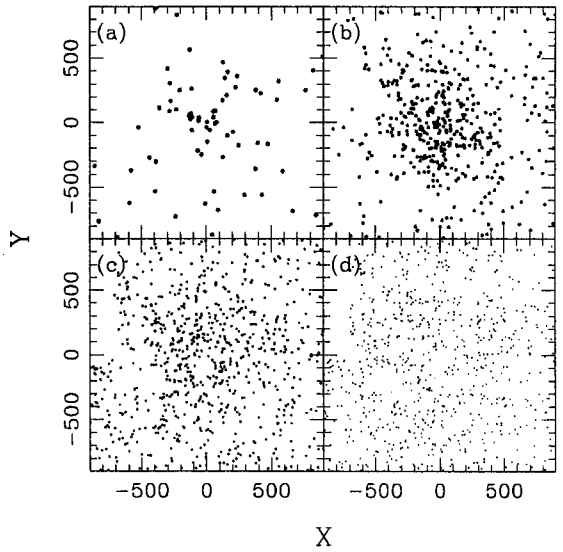

Fig. 6.— The spatial distribution of probable cluster stars which satisfy the photometrical memberships defined in the V vs $V-I$ CMD, complemented by the proper motion memberships for stars brighter than the turn-off point. (a) stars brighter than the turnoff point($V \leq 14.5$), (b) $14.5 < V \leq 16$, (c) $16 < V \leq 17.5$ and (d) $17.5 < V \leq 19.0$.

of previous estimates of the cluster extent show the values around $\sim 5.'5$ (Burkhead 1971, Lindoff 1972). The outer corona of an open cluster is difficult to be identified due to its very low density. As shown in Fig. 5, the stellar density in the outer corona of the cluster ($5.'5 \leq r < 8.'8$) is marginally higher than that of the field region.

(b) Spatial Distribution

Fig. 6 shows the spatial distribution of stars which are located in the photometric regions of the CMD for the probable cluster member stars. For main-sequence stars, the lower envelope of the photometric region is defined by the cluster isochrone whereas the upper envelope is defined by the binary sequence by considering the photometric errors (3σ). For stars brighter than $V = 14.5$, we used the membership probability defined by the proper motion study (Sanders 1972) along with the photometric criteria using the cluster isochrone and photometric errors. We divided the stars into four magnitude groups; $V \leq 14.5$, $14.5 < V \leq 16$, $16 < V \leq 17.5$, and $17.5 < V \leq 19.0$. The stars in the brightest bin, i.e., most massive stars, which have proper motion membership probabilities greater than 0 show a high central concentration, while the stars in the faintest magnitude bin show virtually uniform distribution. These spatial distributions clearly indicate that there is a high degree of mass segregation in NGC 6819. This mass segregation is believed to be due to the dynamical evolution of the cluster because the age of the cluster is much older than the dynamical relaxation time of $\sim 10^8$ yr (Kaliai et al. 2001). Although there seems to be a heavy contamination of field stars in the photometric regions defined for the cluster memberships, the signature of mass segregation in NGC 6819 seems to be a real feature because field stars distribute nearly uniformly across the cluster.

Fig. 7 displays the cumulative radial distribution of probable cluster members. We divide the stars into the four magnitude groups employed in Fig. 6. The effect of mass segregation is also evident in the cumulative distribution, i.e., the half number radius ($\sim$ 2.1 pc) of the upper main-sequence stars ($14.5 < V \leq 16$) is smaller than that ($\sim$ 3.6 pc) of the lower main-sequence stars ($17.5 < V \leq 19.0$). The cumulative distribution for giant stars (plotted by dotted line in Fig. 7) includes several blue straggler candidate stars which are thought to be cluster members by their proper motions (Sanders 1972). The number of blue straggler candidate stars with proper motion membership probability greater than 0 is 14 of which 11 stars have membership probability greater than 0.5. However, the number of blue straggler candidate stars is reduced to 7 if we adopt $P = 0.7$ as the lower limit of the membership probability for cluster stars.

Since half number radius of a cluster strongly depends on the limiting magnitude of the observations, we derived the half mass radius r_h of NGC 6819 by using stellar masses determined from the cluster isochrone. The derived half mass radius of $r_h \approx 2$ pc may be a lower limit because it also depends on the limiting magnitude of the observations. However, the half mass radius derived from the present photometry that reaches

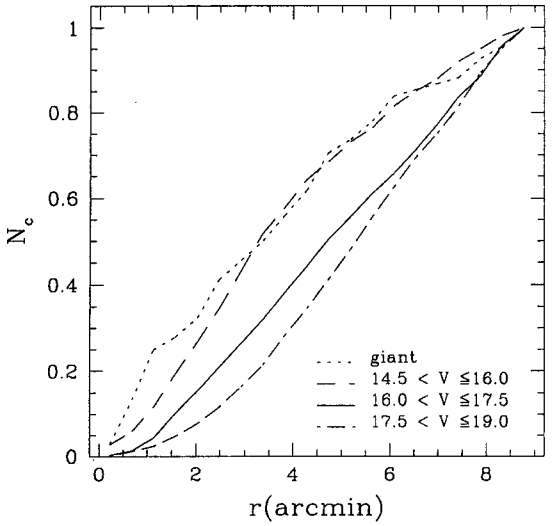

Fig. 7.— Cumulative distribution function of probable cluster members. The stars are divided into four magnitude groups as those of Fig. 6.

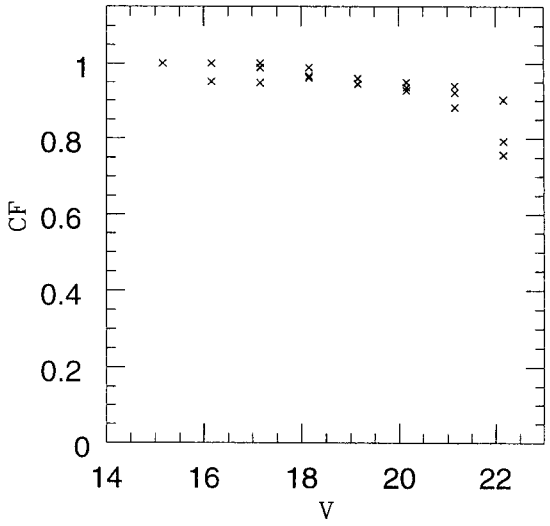

Fig. 8.— Completeness factor of photometry. CF is defined by $CF_V \times CF_I$

down to $M_V \approx 8.5$ seems to be not much different from the real one since stars fainter than $M_V \approx 8.5$ do not significantly contribute to the total mass (Ann & Lee 2002). We derived the dynamical relaxation time by using the equation derived by Spitzer & Hart (1971),

$$t_{rh} = \frac{0.06 M^{1/2} {r_h}^{3/2}}{m G^{1/2} log(0.4N)}$$

where M and m are the total mass of the cluster and the mean stellar mass, respectively, and N is the number of cluster stars. The dynamical relaxation time determined from the present photometry is $\sim 10^8$ yr, which is in a good agreement with that of Kalirai et al. (2001).

V. LUMINOSITY FUNCTIONS

As is well described by Mateo (1988), luminosity function of an open cluster derived from a direct count of the stars in each magnitude bin is affected by many factors of which the incompleteness of photometry as well as field star contamination are the most important ones. Owing to lack of blank field observations, we used the stars located outside $r \approx 8.'8$ to correct field star contamination. Since the cluster seems to extend to $r \approx 9'$, the derived luminosity function is thought to be somewhat underestimated, especially for the faint main-sequence stars.

To correct the incompleteness of photometry, we performed a test based on generating artificial stars on CCD frames which have the same background noise levels as those of the observed frames. We generated artificial stars on the CCD frames using the DAOPHOT utility ADDSTAR and reduce it in the same manner as the observed frames. We used about 100 stars for each magnitude bin. We repeated three trials for V and I frames to get the completeness factors, CF_V and CF_I, respectively, which are defined by the ratios of the recovered stars to the added stars. The final CF was obtained by multiplying CF_V and CF_I to correct the observed luminosity function following Mateo (1988). Fig. 8 shows the variation of CF with magnitudes. We plotted the three trial CFs. Our estimates of CF is $\sim$ 10% smaller than that of Kalirai et al. (2001) due to adding stars on the star-subtracted CCD frames rather than the original CCD frames. It is also worthwhile to note that the true CF of the central region is smaller than that of the outer region due to crowding effect (Mateo 1988). According to Sagar & Richtler (1991) and Sung et al. (1999), the CF of the central region is about two times lower than that of the outer region for stars fainter than $V \approx 19$.

Fig. 9 shows the luminosity function of the probable cluster stars, corrected for the incompleteness of photometry and the field star contamination. Because our corrections are not satisfactory especially for faint stars, the interpretation of the luminosity function in Fig. 9 should be cautious. However, due to the oppoiste direction of the correction terms of field star contamination and incompleteness of photometry, the general shape of the luminosity function in Fig. 9 is thought to be not much different from the true one.

The most prominent feature of the luminosity function of NGC 6819 is the flat distribution of stars in the magnitude range of $3 < M_V < 7$, which corresponds to the magnitude range of the cluster main-sequence, with a slight decreasing trend toward faint magnitudes for the stars fainter than $M_V \approx 5$. Similar flat luminosity function of NGC 6819 was reported by Kalirai et al. (2001). Actually, their luminosity function is

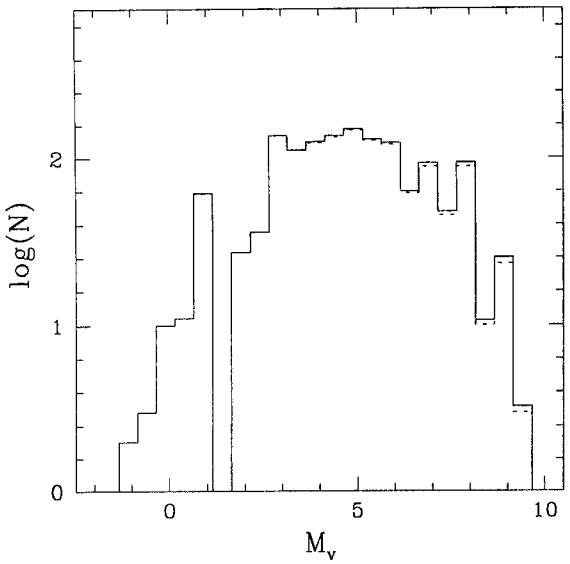

Fig. 9.— The global luminosity function of NGC 6819. It is almost flat between $M_V = 3$ and $M_V = 6$. The dotted line represents the luminosity function before the correction of the incompleteness of photometry. As described in the text, our estimates of the completeness factor (CF) is $\sim 10\%$ smaller than those of Kalirai et al. (2001)

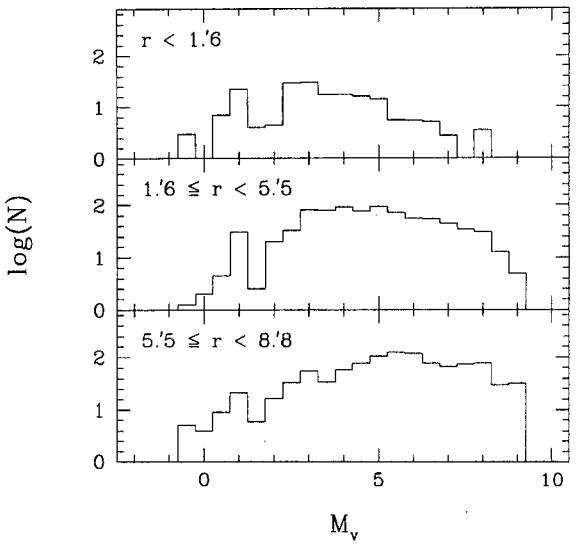

Fig. 10.— The local luminosity functions of NGC 6819. The luminosity function of the core is characterized by the predominance of high mass stars, whereas that of the inner corona is characterized by a flat distribution similar to that of the global luminosity function. The shift between the peak magnitudes of the core and outer corona clearly indicates the presence of mass segregation in NGC 6819.

rather negatively sloped, i.e.,$dN/dM_V < 0$. If we consider that there is a possibility of underestimate of the faintest stars in the derivation of the luminosity function in Fig. 9, the luminosity function of NGC 6819 is almost flat at least for the main-sequence down to $M_V \approx 7$. This flat luminosity function is believed to be caused by the dynamical evolution that results in mass segregation and evaporation of low mass stars. High mass stars are likely to sink to the inner regions, while low mass stars are rambling throughout the cluster. Some of the low mass stars which acquire high enough velocity from equipartion of energy are escaped from the cluster. Because mass segregation means redistribution of stars in the cluster, the flat luminosity function is mainly caused by the evaporation of low mass stars unless its initial mass function has a negative slope assuming Salpeter type initial mass function, i.e., $\Phi(m) \propto m^{-(1+x)}$ with $x < 0$, contrary to the Salpeter (1955) initial mass function ($\Phi(m) \propto m^{-(1+x)}$ with $x = 1.35$).

To see mass segregation more clearly, we derived the local luminosity functions of NGC 6819 by dividing stars into three regions; core ($r < 1.'6$), inner corona ($1.'6 \leq r < 5.'5$), and outer corona ($5.'5 \leq r < 8.'8$), which were defined by the radial surface density distribution in Fig. 5. As shown in Fig. 10, the local luminosity function of the core is much different from that of the outer corona. The luminosity function of the core is characterized by the presence of a peak near $M_V \approx 2.8$ followed by a gradual decrease thereafter, while the luminosity function of the outer corona shows a peak near $M_V \approx 5.5$ with a shallow decrease. Thus, there is a shift in the peak magnitudes of the two luminosity functions, in the sense that from the bright peak magnitude in the core to the faint magnitude in the outer corona. If we consider that CFs of the core region are about two times smaller than those of the outer regions for faint stars ($V \gtrsim 19$) (Sagar & Richtler 1991; Sung et al. 1999), the true luminosity function has a less steep decline after the peak magnitude. However, it is unlikely that the shift in the peak magnitudes can be obliterated by applying correct CF to the luminosity function of the core region. Thus, the local luminosity functions show a clear evidence for mass segregation in NGC 6819.

Since the initial mass function of open clusters is believed to be not much different from that of Salpeter (1955), the decrease of the luminosity functions after peak magnitudes, especially for that of the outer corona, strongly suggests that a large number of low mass stars have escaped from the cluster by acquiring high velocities from encounters with high mass stars. The luminosity function of the inner corona resembles the global luminosity function which is characterized by the flat distribution in the main-sequence range. This resemblance is quite natural since the inner corona seems to be a transition region which should have mixed characteristics.

VI. SUMMARY AND DISCUSSION

We have conducted a deep VI CCD photometry for the field of NGC 6819. The observed area of our photometry is about $18' \times 18'$, centered on the cluster, which covers almost whole of the cluster. We derived the cluster parameters, such as distance and age by fitting the Padova isochrones to the observed stellar distribution in the CMD. Our estimates of the age ($\sim$ 2.5 Gyr) and the distance ($\sim$ 2.3kpc) are in a good agreement with previous ones (Rosvick & VandenBerg 1998; Kalirai et al. 2001).

Analysis of the spatial distribution and luminosity function of probable cluster stars shows that the luminosity function as well as the stellar spatial distribution are much affected by dynamical evolution. Since the age of NGC 6819 is about 10 times larger than its dynamical relaxation time, the cluster seems to be dynamically well relaxed. High mass stars tend to sink to the inner region while low mass stars are likely to be found in the outer regions due to equipartition of energy between stars with different masses.

The global luminosity function of main-sequence of NGC 6819 is almost flat with a slight decrease toward faint magnitudes. The flat luminosity function seems to be the result of evaporation of low mass stars. Mass segregation does affect the spatial distribution of stars but the global luminosity function is not affected by mass segregation itself unless member stars are escaped from the cluster. Without loss of member stars due to evaporation process, the global luminosity function should increase toward faint magnitudes if the initial mass functions of open clusters are assumed to be Salpeter type.

The effects of dynamical evolution in NGC 6819 are more prominent in the local luminosity functions. The luminosity function of the core region ($r < 1.'6$) has a distinct peak at $M_V \approx 2.8$, while the luminosity function of the outer corona ($5.'5 \leq r < 8.'8$) has a less broad peak at $M_V \approx 5.5$. The intermediate region (inner corona) has a flat luminosity function which resembles the global luminosity function. The shift of the peak magnitudes of the luminosity functions is due to dynamical evolution which results in the concentration of high mass stars in the inner regions. The gradual decrease of the luminosity function of the outer corona after the maximum at $M_V \approx 5.5$ is thought to be caused by the evaporation of low mass stars which acquire escape velocity from the encounters with high mass stars during the relaxation process.

For clusters whose ages are much old than their dynamical relaxation times, we expect that the spatial distribution of the cluster stars at the present epoch is much different from the initial spatial distribution due to dynamical evolution through mass segregation and evaporation of low mass stars. Thus, it is quite desirable to estimate the degree of mass segregation and rate of evaporation of low mass stars from observations since they are final results of the dynamical evolution of open clusters.

We would like to thank to the referee (Dr. H. Sung) for several critical comments which improve this paper significantly. This work is supported in part by grant No. R01-1999-00023 from the Korea Science & Engineering Foundation. Kang wants to thank for the grant from the BK21 Program.

REFERENCES

Ann, H. B., & Lee, S. H. 2002, VI CCD photometry of the open cluster NGC 559, JKAS, 35, 29

Anthony-Twarog, B.,& Twarog, B., 1985, Faint stellar photometry in clusters. II - NGC 6791 and NGC 6535, ApJ, 291, 595

Auner, G. 1974, Photographic photometry of the Galactic cluster NGC 6819, A&AS, 13, 143

Bertelli, G., Bressan, A., Chiosi, C., Fagotto, F., & Nasi, E. 1994, Theoretical isochrones from models with new radiative opacities, A&AS 106, 275

Bragaglia, A., Carretta, E., Gratton, R. G., Tosi, M., Bonanno, G., Bruno, P., Cali, A., Claudi, R., Cosentino, R., Desidera, S., Farisato, G., Rebeschini, M., & Scuderi, S., 2001, Metal abundances of red clump stars in open clusters. I. NGC 6819, AJ, 121, 327

Burkhead, M. S. 1971, Photometric observations of the star cluster NGC 6819, AJ, 76, 251

Canterna, R., Geisler, D., Harris, H., Olszewski, E., & Schommer, R. 1986, Washington photometry of open cluster giants the metal-rich clusters, AJ, 92, 79

Christian, C. A. Adams, M., Barnes, J. V., Hayes, D. S., Siegel, M., Butcher, H., & Mould J. R. 1985, Video camera/CCD standard stars (KPNO Video Camera/CCD Standards Consortium), PASP, 97, 363

Dean, J. F., Warren,P. R., & Cousins, A. W. J. 1978, Reddening of Cepheids using BVI photometry, MNRAS, 183, 569

Friel, E. & Janes, K. A. 1993, Metallicities and radial velocities of old open clusters, A&A, 267, 75

Gillaa, S. D. 1993, The evolution of post-main-sequence stars in the old open cluster NGC 6819, Ph.D Thesis, Wyoming Univ.

Kalirai, J. S., Richer, H. B., Fahlman, G. G., Cuiliandre, J.-C., Venture, P., D'Antona, F., & Bertin, E. 2001, The CFHT open star cluster survey. II. Deep CCD photometry of the old open star cluster NGC 6819, AJ, 122, 266

Kaluzny, J., & Shara, M. M. 1988, A CCD Survey for Contact Binaries in Six Open Clusters, AJ, 95, 785

Kang, Y.-W. & Ann, H. B. 2002, In Preparation

King, I. 1962, The structure of star clusters. I. An empirical density aaw, AJ, 67, 471

Landolt, A. U. 1992, $UBVRI$ photometric standard stars in the magnitude range 11.5-16.0 around The celestial equator, AJ, 104, 340

Lindoff, U. 1972, The old open cluster NGC 6819, A&AS, 7, 497

Lyngå G. 1987,"Lund Catalogue of Open Cluster Data", 5th ed.(ADC CD Rom Version)

Mateo, M. 1988, Main-sequence luminosity and initial mass functions of six Magellanic Cloud star clusters ranging in age from 10 Megayears to 2.5 Gigayears, ApJ, 331, 261

Nilakshi, & Sagar, R. 2002, A comprehensive study of the rich open cluster NGC 2099 based on deep *BVI* CCD observations, A&A, 381, 65

Rosvick, J. M., & VandenBerg, D. A. 1998, *BV* photometry for the $\sim$ 2.5 Gyr open cluster NGC 6819: more evidence for convective core overshooting on the main sequence, AJ, 115, 1516

Salpeter, E. E., 1955, The luminosity function and stellar evolution, ApJ, 121, 161

Sanders, W. L. 1972, Membership of the open cluster NGC 6819, A&A, 19, 155

Spitzer, L. Jr., Hart, M. H. 1971, Random gravitational encounters and the evolution of spherical systems. I. Method, ApJ, 164, 399

Sung, H., Bessell, M. S., Lee, H.-W., Kang, Y. H. 1999, *UBVI* CCD photometry of M11 - II. New photometry and surface density profiles, MNRAS, 310, 982

Thogersen, E. N., Friel, E. D., & Fallon, B. V. 1993, Metallicities and velocities of old open clusters, PASP, 105, 1253